Computer Assisted Mechanics and Engineering Sciences, 6: 345–360, 1999.

Ab initio estimates of stability limits on nonlinear load–displacement paths: potential and limitations

Peter Helnwein, Herbert A. Mang and Bernhard Pichler
Institute for Strength of Materials, Vienna University of Technology
Karlsplatz 13, A-1040 Vienna, Austria

(Received March 8, 1999)

In order to avoid a fully nonlinear prebuckling analysis by the finite element method for the mere purpose of obtaining the stability limit in the form of a bifurcation or a snap-through point, this limit may be estimated by means of the solution of a suitable linear eigenvalue problem. What seems to be most suitable in this context, is a consistent linearization of the mathematical formulation of the static stability condition. It can be interpreted as the stability criterion for the tangent to the load–displacement diagram at a known equilibrium state in the prebuckling domain. Based on this linearization, higher-order estimates of the stability limit can be obtained from scalar postcalculations. Unfortunately, the order of such an estimate is only defined in an asymptotic sense. Nevertheless, for many engineering structures the geometric nonlinearity in the prebuckling domain is moderate. In this case, the general information from asymptotic analysis is frequently relevant for the entire prebuckling domain. This allows good *ab initio* estimates of stability limits based on nonlinear load–displacement paths.

The nucleus of this article is the discussion of the potential and the limitations of determination of stability limits based on *ab initio* estimates of nonlinear load–displacement paths. The theoretical findings are corroborated by the results from a comprehensive numerical study.

1. Introduction

Determination of stability limits (bifurcation or limit points) on nonlinear load–displacement paths of elastic structures requires use of a geometrically nonlinear theory. With the help of the principle of virtual displacements and the Finite Element Method (FEM), the respective system of nonlinear differential equations is converted to a system of nonlinear algebraic equations. The incremental-iterative solution of this system of equations must include checks for stability limits.

In order to avoid a fully nonlinear prebuckling analysis for the mere purpose of obtaining the stability limit, estimates of this limit based on the solution of linear eigenvalue problems have frequently been used [2, 3, 4, 5, 11]. Mang and Helnwein, e.g., have suggested a consistent linearization of the mathematical formulation of the static stability condition [7, 12, 13, 14]. It can be interpreted as the stability criterion for the tangent to the load–displacement diagram at a known equilibrium state in the stable prebuckling domain. Based on this linearization, higher-order estimates of the stability limit can be obtained from a scalar postcalculation.

Unfortunately, the order of such an estimate is only defined in an asymptotic sense. Nevertheless, for many engineering structures the geometric nonlinearity in the prebuckling domain is moderate [6]. In this case, the general information from asymptotic analysis is frequently relevant for the entire prebuckling domain. This allows good *ab initio* estimates of stability limits on nonlinear load–displacement paths.

However, the optimum estimate for a snap-through point differs from the optimum estimate for a bifurcation point [8]. Hence, an *ab initio* assessment of the kind of stability limit is necessary. A respective *ab initio* condition will be presented in the paper. Moreover, a condition for the reliability

of estimates on nonlinear load–displacement paths will be proposed. They were tested numerically by Pichler [15].

The theoretical findings are corroborated by the results from a comprehensive numerical study based on an example problem analyzed by Sabir and Lock [16]. This example serves as a benchmark for shell theories and finite element formulations, see, e.g., Simo et al. [19].

2. Theoretical background for the estimation of stability limits

The problem investigated in this paper is estimation of stability limits on nonlinear load–displacement paths of elastic structures. The applied load is assumed to be static and conservative (Hence, follower loads are admitted so long as they have a potential). The analyses will be carried out by means of the finite element method (FEM). The loading of the structure is assumed to be proportional to a reference load:

$$\mathbf{P} = \lambda \bar{\mathbf{P}} \,, \tag{1}$$

where $\mathbf{P}$ is the vector of the total nodal forces, $\bar{\mathbf{P}}$ is the vector of reference nodal forces and λ is a dimensionless load parameter.

The mathematical condition for a static stability limit can be written as [8, 20]

$$\mathcal{G}(\lambda_S, \delta\mathbf{q}) = \mathbf{K}_T(\mathbf{q}(\lambda_S))\,\delta\mathbf{q} = \mathbf{0} \,, \tag{2}$$

where $\mathbf{K}_T$ is the standard tangent stiffness matrix, $\mathbf{q}$ is the vector of nodal displacements, λ_S is the value of the load parameter λ at the stability limit and $\delta\mathbf{q}$ is a vector describing the buckling mode. The notion *stability limit* is solely used for the solution of (2) corresponding to the smallest load level, λ_S. (2) is a nonlinear eigenvalue problem with λ_S and $\delta\mathbf{q}$ representing the eigenvalue and eigenvector, respectively. The dimension of the problem is defined by the total number N of degrees of freedom of the FE-model of the structure to be investigated.

2.1. Estimation for the stability limit

In order to avoid the solution of the nonlinear eigenvalue problem (2), several linear eigenvalue problems serving as substitute problems of the actual problem were reported in the literature. For a review see Helnwein [6]. In the vicinity of the stability limit they provide estimates of this limit.

In what follows, the so-called consistently linearized eigenvalue problem [8]

$$\left[\mathbf{K}_T + \omega\,\mathbf{K}_T'\right]\delta\mathbf{q}^* = \mathbf{0} \tag{3}$$

will be used as the basis for the development of estimation functions for λ_S. $\mathbf{K}_T' = d\mathbf{K}_T/d\lambda$ is the derivative of $\mathbf{K}_T$ with respect to the load parameter λ, ω is the eigenvalue and $\delta\mathbf{q}^*$ is the corresponding eigenvector. The notation $\delta\mathbf{q}^*$ instead of $\delta\mathbf{q}$ in (2) should indicate that, because of linearization of (2), $\delta\mathbf{q}^*(\lambda)$ is an approximation of $\delta\mathbf{q}$. The function

$$\lambda^*(\lambda) = \lambda + \omega \tag{4}$$

is the expected estimate of λ_S at a given load level $\lambda < \lambda_S$. Since it is based on the eigenvalue ω, it may be referred to as eigenvalue-function.

Derivation of (3) with respect to λ, using a prime ($'$) as an abbrevation for $d/d\lambda$, yields

$$\left[\lambda^{*\prime}\,\mathbf{K}_T' + \omega\,\mathbf{K}_T''\right]\delta\mathbf{q}^* + \left[\mathbf{K}_T + \omega\,\mathbf{K}_T'\right]\delta\mathbf{q}^{*\prime} = \mathbf{0} \,. \tag{5}$$

Premultiplying (5) by the eigenvector $\delta\mathbf{q}^{*T}$ and making use of (3) yields

$$\lambda^{*\prime} = -\omega\,\frac{\delta\mathbf{q}^{*T}\mathbf{K}_T''\delta\mathbf{q}^*}{\delta\mathbf{q}^{*T}\mathbf{K}_T'\delta\mathbf{q}^*} \,. \tag{6}$$

Thus, not only the value of the estimation function λ^* can be obtained by means of solving the eigenvalue problem (3) but also the slope of this function is available from a scalar postcalculation according to (6). However, computation of $\lambda^{*\prime}$ requires knowledge of $\mathbf{K}_T''$ which depends on $\mathbf{q}'$ and $\mathbf{q}''$. In order to be able to compute $\mathbf{q}''$, the rate form of the equilibrium equations for the discretized continuum must be differentiated with respect to λ:

$$\mathbf{K}_T\, d\mathbf{q} = d\lambda\, \bar{\mathbf{P}} \quad \longrightarrow \quad \mathbf{K}_T\, \mathbf{q}' = \bar{\mathbf{P}} \quad \longrightarrow \quad \mathbf{K}_T\, \mathbf{q}'' = -\mathbf{K}_T'\, \mathbf{q}' \tag{7}$$

2.2. Error evaluation

The asymptotic quality of a wide range of estimation functions can be evaluated by means of an asymptotic approach presented by Helnwein and Mang [8]. This can be achieved by means of the estimation error $\mathcal{E}_\lambda = \lambda^*(\lambda) - \lambda_S$. This error can be expressed as a Taylor series at the critical point:

$$\mathcal{E}_\lambda = \sum_{k=1}^{\infty} \frac{1}{k!} \left.\frac{\mathrm{d}^k \lambda^*}{\mathrm{d}\lambda^k}\right|_{\lambda_S} (\lambda - \lambda_S)^k = \left.\lambda^{*\prime}\right|_{\lambda_S} (\lambda - \lambda_S) + \frac{1}{2} \left.\lambda^{*\prime\prime}\right|_{\lambda_S} (\lambda - \lambda_S)^2 + \dots \,. \tag{8}$$

Based on the coefficients in (8), the order of the error $\mathcal{E}_\lambda$ was defined as [8]

$$\mathcal{O}(\mathcal{E}_\lambda) = \min \left\{ k \in \mathbb{N}^+ \,\middle|\, \lim_{\lambda \to \lambda_S} \frac{\mathrm{d}^k \lambda^*}{\mathrm{d}\lambda^k} \neq 0 \right\} \,. \tag{9}$$

The higher the order of the error, the larger the interval $[\lambda < \lambda_S, \lambda_S]$ wherein λ^* is a suitable estimate of λ_S.

2.3. Higher order estimation of stability limits

Making use of the eigenvalue ω obtained from (3) and the slope $\lambda^{*\prime}$ of the estimation function according to (6), other estimation functions can be determined.

Extrapolation along the tangent of the estimation function λ^* according to (4) yields [14]

$$\tilde{\lambda} = \lambda + \frac{\omega}{1 - \lambda^{*\prime}} \,. \tag{10}$$

Making use of results from the evaluation of the order of the error of $\lambda^*(\lambda)$ for bifurcation points permits a quadratic extrapolation for λ^*. The respective estimation function is obtained as [6]

$$\lambda^{**} = \lambda + \frac{\omega}{1 - \frac{1}{2}\lambda^{*\prime}} \,. \tag{11}$$

An assessment of the quality of the estimation functions λ^*, $\tilde{\lambda}$ und λ^{**} by means of the asymptotic approach and the definition (9) was carried out by Helnwein and Mang [8]. As apposed to bifurcation points, snap-through points are singular points of the curves $\lambda^*(\lambda)$. Thus, the investigation of the order of the estimation error needs to be performed independently for bifurcation points and snap-through points.

Table 1 contains the obtained order of the estimation error for the mentioned estimation functions as derived by Helnwein and Mang [8]. The boxes in Table 1 mark the best choices (in an asymptotic sense) out of the considered estimation functions. The order of the estimation error of these functions is higher than the one of the original eigenvalue function λ^*. Thus, they will be referred to as *higher-order estimations.*

Since the asymptotic properties of λ^{**} are optimal for bifurcation points, whereas the asymptotic properties of $\tilde{\lambda}$ are optimal for snap-through points, an *a priori* indicator of the type of stability limit is required.

Table 1. Order of the estimation error for the consistently linearized eigenproblem and two modes of higher-order estimation, both for bifurcation and snap-through points

	see	bifurcation point	snap-through point
$\lambda^*(\lambda)$	(4)	2	1
$\tilde{\lambda}(\lambda)$	(10)	2	$\boxed{2}$
$\lambda^{**}(\lambda)$	(11)	$\boxed{3}$	1

It is given as follows:

$$\delta\mathbf{q}^* \cdot \bar{\mathbf{P}}|_{\lambda=0} = 0 \ldots \text{ for a bifurcation point}$$
$$\delta\mathbf{q}^* \cdot \bar{\mathbf{P}}|_{\lambda=0} \neq 0 \ldots \text{ for a snap-through point}$$

These indicators are based on the fact that $\delta\mathbf{q}^*\bar{\mathbf{P}}|_{\lambda=0}$ is a necessary *a priori* condition for loss of stability by bifurcation buckling. (However, it is not a sufficient condition, because there may be modes satisfying this condition although loss of stability occurs by snap-through or does not occur at all. The respective modes are obviously irrelevant for these situations.) It is worth mention that, provided the aforementioned condition holds at $\lambda = 0$, it will hold in the entire prebuckling domain and, obviously, at the bifurcation point. This follows from decomposition of the derivatives of the orthogonality conditions $(\delta\mathbf{q}_i^{*T}\mathbf{K}_T\,\delta\mathbf{q}_j^*) = 0$ and $(\delta\mathbf{q}_i^{*T}\mathbf{K}_T'\,\delta\mathbf{q}_j^*) = 0$, $i \neq j$, with respect to λ for such modes.

On the basis of this condition the following angle is defined:

$$\alpha^* = \arcsin\frac{|\delta\mathbf{q}^* \cdot \bar{\mathbf{P}}|}{\|\delta\mathbf{q}^*\|\,\|\bar{\mathbf{P}}\|}\,, \qquad \alpha^* \in [0, \frac{\pi}{2}] \subset \mathbb{R}\,. \tag{12}$$

At the stability limit, $\alpha^* = 0$ indicates a bifurcation point and $\alpha^* > 0$ indicates a snap-through point. Hence, the angle α^* represents the deviation of the eigenvector $\delta\mathbf{q}^*$ from orthogonality to $\bar{\mathbf{P}}$.

Because of the aforementioned orthogonality of "bifurcation modes" in the entire prebuckling domain, $\alpha^* = 0$ should theoretically also hold at $\lambda < 0$ for such modes. A series of test examples concerning trusses, plane frames, and shells has resulted in the following numerical criterion [6]:

$$\alpha^* < 0.2° : \text{bifurcation point}$$
$$\alpha^* > 1.0° : \text{snap-through point}$$

For values of α^* in the range $\alpha^* \in [0.2°, 1.0°]$ it is necessary to consider the values of α^* for 3 to 5 of the lowest eigenvalues in order to classify "small" values of α^* ($\rightarrow$ bifurcation point) relative to "large" values ($\rightarrow$ snap-through point). The test examples have shown that always $\alpha^*_{\text{snap-through}}/\alpha^*_{\text{bifurcation}} > 10$. The mentioned problem only occurs for large values of N and for the case of iterative computation of eigenvectors at a low level of accuracy. It is re-emphasized that the *a priori* identification of "bifurcation modes" only indicates the possibility of loss of stability by means of bifurcation.

3. Development of an indicator for the reliability of estimates of the stability limit

The main purpose of the dissertation by Helnwein [6] was the development of *ab initio* estimations of the stability limit by means of a suitable linear eigenvalue problem. The analytical and numerical investigations have shown that the usefulness of the estimation functions λ^*, $\tilde{\lambda}$ and λ^{**} may be restricted to a more or less narrow subdomain of the prebuckling domain before the stability limit. Nevertheless, tests on a relatively wide range of engineering structures have shown that *ab initio* estimations of the stability limit can be of a remarkably high quality. Hence, what is needed is an indicator for the reliability of an *ab initio* estimation for a certain structure.

In order to obtain such an indicator, further information on the structural behavior is needed. The basis of this information is the first derivative of the estimated eigenvector $\delta\mathbf{q}^*$ with respect to λ. This vector, denoted by $\delta\mathbf{q}^{*\prime}$, is the only quantity in (5) which was not computed so far because it was not needed for the evaluation of (4), (10) and (11).

3.1. Derivative of the eigenvector with respect to the load parameter

In this section, two modes of normalization of the eigenvector are taken into account. The first mode is based on the Euclidean norm of the eigenvector $\delta\mathbf{q}^*$. It is defined as

$$\delta\mathbf{q}^* \cdot \delta\mathbf{q}^* = \delta\mathbf{q}^{*T}\delta\mathbf{q}^* = +1 \; . \tag{13}$$

The second mode of normalization is based on the quadratic form involving $\mathbf{K}_T'$, i.e., the second matrix in the equation of definition of the consistently linearized eigenvalue problem (3). This quadratic form is defined as

$$\delta\mathbf{q}^{*T}\mathbf{K}_T'\delta\mathbf{q}^* = \mp 1 \; . \tag{14}$$

In the prebuckling domain, the negative sign in (14) is relevant for positive eigenvalues ω while the positive sign holds for negative values of ω.

In the following, both modes of normalization will be used. The symbols $\delta\hat{\mathbf{q}}$ and $\delta\hat{\mathbf{q}}'$ are introduced to denote the eigenvector and its derivative, respectively, satisfying (13) and the derivative of (13) with respect to λ.

Assuming that the slope $\lambda^{*\prime}$ has been computed according to (6), $\delta\mathbf{q}^{*\prime}$ is the only unknown in (5). Because of (3), the matrix

$$\mathbf{K}_T^* = \left[\mathbf{K}_T + \omega\,\mathbf{K}_T'\right] \tag{15}$$

is singular. If ω is a single eigenvalue of (3), the rank of the matrix $\mathbf{K}_T^*$ is $N-1$. Thus, an additional equation is needed for the evaluation of $\delta\mathbf{q}^{*\prime}$. This equation is obtained by differentiating the normalization condition (13) for $\delta\hat{\mathbf{q}}$ and (14) for $\delta\mathbf{q}^*$, respectively. Use of the (13) yields

$$\delta\hat{\mathbf{q}}^T\delta\hat{\mathbf{q}}' = 0 \; , \tag{16}$$

whereas use of (14) gives

$$2\,\delta\mathbf{q}^{*T}\mathbf{K}_T'\delta\mathbf{q}^{*\prime} + \delta\mathbf{q}^{*T}\mathbf{K}_T''\delta\mathbf{q}^* = 0 \; . \tag{17}$$

Because of (3), the vectors $\delta\mathbf{q}^*$ and $\delta\hat{\mathbf{q}}$ are related as follows:

$$\delta\mathbf{q}^* = \beta\,\delta\hat{\mathbf{q}} \; , \tag{18}$$

i.e., they only differ by their length. Considering (13), the scalar factor β can be obtained from the scalar product $\delta\mathbf{q}^* \cdot \delta\mathbf{q}^*$ as follows:

$$\delta\mathbf{q}^* \cdot \delta\mathbf{q}^* = \beta^2\,\delta\hat{\mathbf{q}} \cdot \delta\hat{\mathbf{q}} = \beta^2 \; . \tag{19}$$

The corresponding relation between the derivatives $\delta\mathbf{q}^{*\prime}$ and $\delta\hat{\mathbf{q}}'$ is computed with the help of the first derivative of (18) with respect to λ. It is obtained as follows:

$$\delta\mathbf{q}^{*\prime} = \beta'\,\delta\hat{\mathbf{q}} + \beta\,\delta\hat{\mathbf{q}}' = \beta\left(\delta\hat{\mathbf{q}}' + (\ln\beta)'\,\delta\hat{\mathbf{q}}\right) = \beta\,\delta\hat{\mathbf{q}}' + (\ln\beta)'\,\delta\mathbf{q}^* \; . \tag{20}$$

Substitution of (18) and (20) into (5) and division of the result by β yields

$$\left\{\left[\lambda^{*\prime}\mathbf{K}_T' + \omega\,\mathbf{K}_T''\right]\,\delta\hat{\mathbf{q}} + \left[\mathbf{K}_T + \omega\,\mathbf{K}_T'\right]\,\delta\hat{\mathbf{q}}'\right\} + (\ln\beta)'\left\{\left[\mathbf{K}_T + \omega\,\mathbf{K}_T'\right]\,\delta\hat{\mathbf{q}}\right\} = \mathbf{0} \; . \tag{21}$$

Because of (3), the last term in (21) is equal to $\mathbf{0}$. Thus, Eq. (21) remains formally identical to (5), although (20) is not trivial.

Rewriting (6) as

$$\delta\mathbf{q}^{*T}\mathbf{K}_T''\delta\mathbf{q}^* = -\frac{\lambda^{*\prime}}{\omega}\,\delta\mathbf{q}^{*T}\mathbf{K}_T'\delta\mathbf{q}^* \tag{22}$$

and substituting this relation into (17) yields

$$\left(2\,\omega\,\delta\mathbf{q}^{*\prime} - \lambda^{*\prime}\,\delta\mathbf{q}^*\right)\mathbf{K}_T'\,\delta\mathbf{q}^* = 0\;. \tag{23}$$

Because of (3) and of the symmetry of $\mathbf{K}_T$ and $\mathbf{K}_T'$, the following relations between the first eigenvector $\delta\mathbf{q}_1^* = \delta\mathbf{q}^*$ and the eigenvectors $\delta\mathbf{q}_k^*$, $k \geq 2$, hold:

$$\delta\mathbf{q}_k^{*T}\,\mathbf{K}_T\,\delta\mathbf{q}^* = 0 \quad \text{and} \quad \delta\mathbf{q}_k^{*T}\,\mathbf{K}_T'\,\delta\mathbf{q}^* = 0 \quad \forall k \geq 2\;(\omega_k \neq \omega)\;. \tag{24}$$

Because of (14) and (24), it follows from (23) that the vector $(2\,\omega\,\delta\mathbf{q}^{*\prime} - \lambda^{*\prime}\,\delta\mathbf{q}^*)$ is an element of the $(N-1)$-dimensional subspace $\mathcal{T}$ given as

$$\mathcal{T} = \text{span}\,\{\delta\mathbf{q}_2^*, \ldots, \delta\mathbf{q}_k^*, \ldots, \delta\mathbf{q}_N^*\} \subset \mathbb{R}^N\;. \tag{25}$$

Substitution of $\delta\mathbf{q}^{*\prime}$ into (23) by means of (20) yields

$$\left[2\,\omega\,(\ln\beta)' - \lambda^{*\prime}\right]\delta\mathbf{q}^{*T}\mathbf{K}_T'\delta\mathbf{q}^* + 2\,\omega\,\beta\,\delta\mathbf{q}^{*T}\mathbf{K}_T'\delta\hat{\mathbf{q}}' = 0\;. \tag{26}$$

Solving (26) for $(\ln\beta)'$ and making use of (14) and (18) leads to the following alternatives for the description of $(\ln\beta)'$:

$$\begin{aligned}(\ln\beta)' &= \frac{\lambda^{*\prime}}{2\,\omega} - \beta\,\frac{\delta\mathbf{q}^{*T}\mathbf{K}_T'\delta\hat{\mathbf{q}}'}{\delta\mathbf{q}^{*T}\mathbf{K}_T'\delta\mathbf{q}^*} = \frac{\lambda^{*\prime}}{2\,\omega} \pm \beta\,\delta\mathbf{q}^{*T}\mathbf{K}_T'\delta\hat{\mathbf{q}}' \\ &= \frac{\lambda^{*\prime}}{2\,\omega} - \frac{\delta\hat{\mathbf{q}}^T\mathbf{K}_T'\delta\hat{\mathbf{q}}'}{\delta\hat{\mathbf{q}}^T\mathbf{K}_T'\delta\hat{\mathbf{q}}}\;.\end{aligned} \tag{27}$$

Substitution of (27) into (20) permits transforming $\delta\hat{\mathbf{q}}'$ to $\delta\mathbf{q}^{*\prime}$.

3.1.1. Notes on the computational implementation

Because of the singularity of $\mathbf{K}_T^* = [\mathbf{K}_T + \omega\,\mathbf{K}_T']$ in (5), $\delta\mathbf{q}^{*\prime}$ cannot be computed directly by inversion of $\mathbf{K}_T^*$. $\delta\mathbf{q}^{*\prime}$ could, however, be determined by replacing a suitable row in the system of Eqs. (5) by either (16) or (17). This strategy has the disadvantage that the symmetry as well as the bandedness of $\mathbf{K}_T^*$ is lost. Thus, the data structure for matrix storage would have to be changed. Furthermore, a solver for non-symmetric systems of equations would be needed.

In order to obtain a symmetric coefficient matrix, the rank deficiency of $\mathbf{K}_T^*$ may be removed by replacing $\mathbf{K}_T^*$ in (5) by the matrix

$$\mathbf{A} = \mathbf{K}_T^* + c\,\delta\hat{\mathbf{q}}\,\delta\hat{\mathbf{q}}^T\;. \tag{28}$$

In (28), $c \in \mathbb{R}^+$ is an arbitrary constant.

Defining the vector

$$\mathbf{b} = -\left[\lambda^{*\prime}\,\mathbf{K}_T' + \omega\,\mathbf{K}_T''\right]\delta\hat{\mathbf{q}} = -\mathbf{K}_T^{*\prime}\delta\hat{\mathbf{q}}\;, \tag{29}$$

the modified Eq. (5) and its solution, respectively, can formally be written as

$$\mathbf{A}\mathbf{x} = \mathbf{b} \quad \Rightarrow \quad \mathbf{x} = \mathbf{A}^{-1}\mathbf{b}\;. \tag{30}$$

Premultiplication of (5) by $\delta\hat{\mathbf{q}}^T$ and use of (3) and (29) yields

$$\delta\hat{\mathbf{q}}^T \left[\lambda^{*\prime}\,\mathbf{K}_T' + \omega\,\mathbf{K}_T''\right] \delta\hat{\mathbf{q}} = -\delta\hat{\mathbf{q}}^T\mathbf{b} = 0 \quad \Rightarrow \quad \delta\hat{\mathbf{q}} \perp \mathbf{b}\,. \tag{31}$$

Premultiplying the first of the two relations (30) by $\delta\hat{\mathbf{q}}^T$ gives

$$\delta\hat{\mathbf{q}}^T\mathbf{A}\mathbf{x} = \delta\hat{\mathbf{q}}^T\mathbf{b}\,. \tag{32}$$

Substitution of (28) into (32) yields

$$\delta\hat{\mathbf{q}}^T[\mathbf{K}_T^* + c\,\delta\hat{\mathbf{q}}\delta\hat{\mathbf{q}}^T]\mathbf{x} = \delta\hat{\mathbf{q}}^T\mathbf{b}\,. \tag{33}$$

Because of $\mathbf{K}_T^*\,\delta\hat{\mathbf{q}} = \mathbf{0}$ and $\delta\hat{\mathbf{q}} \perp \mathbf{b}$, the solution vector $\mathbf{x}$ is orthogonal to $\delta\hat{\mathbf{q}}$. According (13) and (16), $\delta\hat{\mathbf{q}}'$ is also orthogonal to $\delta\hat{\mathbf{q}}$. Thus,

$$\delta\hat{\mathbf{q}}' = \mathbf{x}\,. \tag{34}$$

Hence, $\delta\hat{\mathbf{q}}'$ can be obtained by means of relation (30).

Although $\mathbf{A}$ is symmetric, it is generally fully populated because of the term $\delta\hat{\mathbf{q}}\,\delta\hat{\mathbf{q}}^T$ in (28). In order to preserve the bandedness of the structure of $\mathbf{K}_T^*$, an iterative procedure is derived. It starts with an approximation for $\mathbf{A}$ as

$$\bar{\mathbf{A}} = \mathbf{K}_T^* + c\,\mathbf{e}_k\,\mathbf{e}_k^T \tag{35}$$

where $\mathbf{e}_k$ is a unit vector, the k-th component of which is 1, i.e.,

$$\mathbf{e}_k = [0,\ldots,0,1,0,\ldots,0]^T. \tag{36}$$

This is equivalent to setting the k-th diagonal element of $\mathbf{D}$ in an $\mathbf{LDL}^T$-decomposition [1] of the singular matrix $\mathbf{K}_T^*$ equal to c which should be chosen as a small positive number, instead of $c \in \mathbb{R}^+$ as required by (28). Practically, k is the number of the first diagonal element which becomes zero (or smaller than a prespecified tolerance) during the decomposition process. For a single eigenvalue, i.e., for a rank deficiency of 1, this occurs just once.

Substitution of $\mathbf{A}$ in (30) by $\bar{\mathbf{A}}$ according to (35) enables computation of an approximation for $\delta\hat{\mathbf{q}}'$ as described by the following two steps. In the first step a vector

$$\bar{\mathbf{x}} = \bar{\mathbf{A}}^{-1}\mathbf{b} \tag{37}$$

is obtained from inversion of $\bar{\mathbf{A}}$. The second step consists of satisfaction of (16). For this purpose a projection of the vector $\bar{\mathbf{x}}$ onto the hyperplane perpendicular to the eigenvector $\delta\hat{\mathbf{q}}$ is performed. The obtained projection is used as the first approximation for $\delta\hat{\mathbf{q}}'$, i.e.,

$$\delta\hat{\mathbf{q}}'_{(1)} = \left(\mathbb{I} - \delta\hat{\mathbf{q}}\,\delta\hat{\mathbf{q}}^T\right)\bar{\mathbf{x}}\,. \tag{38}$$

The quality of this approximation can be checked by means of Eq. (5). This relation is used for computation of a residual vector:

$$\mathbf{R}(\delta\hat{\mathbf{q}}') = \mathbf{b} - \mathbf{K}_T^*\,\delta\hat{\mathbf{q}}' = -\left[\lambda^{*\prime}\,\mathbf{K}_T' + \omega\,\mathbf{K}_T''\right]\delta\hat{\mathbf{q}} - \left[\mathbf{K}_T + \omega\,\mathbf{K}_T'\right]\delta\hat{\mathbf{q}}'\,. \tag{39}$$

Then, the Euclidean norm is checked against a small positive value ε. For the k-th iterative step this norm is obtained as

$$\frac{\|\mathbf{R}(\delta\hat{\mathbf{q}}'_{(k)})\|}{\|\delta\hat{\mathbf{q}}\|} = \|\mathbf{R}(\delta\hat{\mathbf{q}}'_{(k)})\| \le \varepsilon\,. \tag{40}$$

ε is a tolerance value defined by the user. For computations based on double precision floating point numerics, a value of $\varepsilon = 10^{-12}$ has led to reliable and efficient results for $\delta\hat{\mathbf{q}}'$ and $\delta\mathbf{q}^{*\prime}$, respectively.

If (40) is not satisfied, a better approximation is obtained from

$$\delta\hat{\mathbf{q}}'_{(k+1)} = \delta\hat{\mathbf{q}}'_{(k)} + \left(\mathbb{I} - \delta\hat{\mathbf{q}}\,\delta\hat{\mathbf{q}}^T\right)\bar{\mathbf{A}}^{-1}\,\mathbf{R}(\delta\hat{\mathbf{q}}'_{(k)}) \; . \tag{41}$$

This formula combines both steps described by (37) and (38). Finally, the quality of the result is checked. This procedure was tested for several structural problems. In general, it converged within one to two cycles. The maximum number of cycles was 3.

The computational effort for the described procedure consists of a single triangular decomposition of $\bar{\mathbf{A}}$ and a maximum of three iteration steps consisting of computations of the residual vector $\mathbf{R}$ and back-substitution with $\mathbf{R}$ as the right-hand-side vector.

The transformation from $\delta\hat{\mathbf{q}}$ to $\delta\mathbf{q}^*$ and $\delta\hat{\mathbf{q}}'$ to $\delta\mathbf{q}^{*\prime}$ is done by means of (18) and (20), respectively. The scalar factor β in (18) can be obtained by substitution of (18) into (14) as

$$\delta\mathbf{q}^{*T}\mathbf{K}'_T\delta\mathbf{q}^* = \beta^2\,\delta\hat{\mathbf{q}}^T\mathbf{K}'_T\delta\hat{\mathbf{q}} = \mp 1 \quad \Rightarrow \quad \beta = \frac{1}{\sqrt{|\delta\hat{\mathbf{q}}^T\mathbf{K}'_T\delta\hat{\mathbf{q}}|}} \; . \tag{42}$$

Substituting (42) into (27) yields the coefficent $(\ln\beta)'$:

$$(\ln\beta)' = \frac{\lambda^{*\prime}}{2\,\omega} \pm \beta^2\,\delta\hat{\mathbf{q}}^T\mathbf{K}'_T\delta\hat{\mathbf{q}}' \tag{43}$$

The vector $\delta\mathbf{q}^{*\prime}$ is then obtained from (20). The sign in (43) is the opposite of the sign of the quadratic form defining the normalization, i.e., the sign of $\delta\hat{\mathbf{q}}^T\mathbf{K}'_T\delta\hat{\mathbf{q}}$.

3.2. Indicator functions for the reliability of estimates

The basic idea for the definition of such an indicator function is consideration of the derivative of the eigenvector with respect to the load parameter. It is motivated by the fact that, on the one hand, this vector contains information about the development of the structural behavior but, on the other hand, it does not appear in the previously proposed estimation functions. A detailed investigation concerning the suitability of such indicator functions is the main topic of the diploma thesis of Pichler [15]. In the following, the basic ideas of this work will be given.

A reliability indicator can be obtained, e.g., by premultiplying (5) by $\delta\mathbf{q}^{*\prime T}$ and writing the result as

$$\omega\,\delta\mathbf{q}^{*T}\mathbf{K}''_T\delta\mathbf{q}^{*\prime} = -\lambda^{*\prime}\,\delta\mathbf{q}^{*T}\mathbf{K}'_T\delta\mathbf{q}^{*\prime} - \delta\mathbf{q}^{*\prime T}\left[\mathbf{K}_T + \omega\,\mathbf{K}'_T\right]\delta\mathbf{q}^{*\prime} \; . \tag{44}$$

Dividing (44) by ω and making use of (17), the bilinear form $\delta\mathbf{q}^{*T}\mathbf{K}'_T\delta\mathbf{q}^{*\prime}$ can be expressed by means of the already computed quadratic form $\delta\mathbf{q}^{*T}\mathbf{K}''_T\delta\mathbf{q}^*$. Thus, $\delta\mathbf{q}^{*T}\mathbf{K}''_T\delta\mathbf{q}^{*\prime}$ may be written as

$$\delta\mathbf{q}^{*T}\mathbf{K}''_T\delta\mathbf{q}^{*\prime} = \frac{\lambda^{*\prime}}{2\,\omega}\,\delta\mathbf{q}^{*T}\mathbf{K}''_T\delta\mathbf{q}^* - \frac{1}{\omega}\,\delta\mathbf{q}^{*\prime T}\left[\mathbf{K}_T + \omega\,\mathbf{K}'_T\right]\delta\mathbf{q}^{*\prime} \; . \tag{45}$$

Using (22) and (14), the ratio $\lambda^{*\prime}/\omega$ can be expressed by means of $\delta\mathbf{q}^{*T}\mathbf{K}''_T\delta\mathbf{q}^*$. Consequently, (45) may be rewritten as

$$\delta\mathbf{q}^{*T}\mathbf{K}''_T\delta\mathbf{q}^{*\prime} = \pm\frac{1}{2}\,(\delta\mathbf{q}^{*T}\mathbf{K}''_T\delta\mathbf{q}^*)^2 - \frac{1}{\omega}\,\delta\mathbf{q}^{*\prime T}\left[\mathbf{K}_T + \omega\,\mathbf{K}'_T\right]\delta\mathbf{q}^{*\prime} \; . \tag{46}$$

In the prebuckling domain the positive sign in (46) holds for $\omega > 0$, whereas the negative sign holds for $\omega < 0$. For the smallest positive eigenvalue ω, the matrix $[\mathbf{K}_T + \omega\,\mathbf{K}'_T]$ is positive semi-definite. Thus, $\delta\mathbf{q}^{*\prime T}\left[\mathbf{K}_T + \omega\,\mathbf{K}'_T\right]\delta\mathbf{q}^{*\prime} \geq 0$.

Considering only the smallest positive eigenvalue, which is the basis for the estimation of the stability limit, both terms in (46) are ≥ 0 in the prebuckling domain. Since the value of $\delta\mathbf{q}^{*T}\mathbf{K}_T''\delta\mathbf{q}^{*\prime}$ is computed as the difference of two nonnegative values, both signs are possible. At the stability limit and in a subregion of the prebuckling domain before this limit, the bilinear form according to (46) must be positive. This property was the rationale for introducing this bilinear form as the basis for a reliability indicator of *ab initio* estimates of stability limits [15].

An alternative reliability indicator may be obtained by means of the scalar product $\delta\mathbf{q}^* \cdot \delta\mathbf{q}^{*\prime}$ or by the ratio $(\delta\mathbf{q}^{*\prime} \cdot \delta\mathbf{q}^{*\prime})/(\delta\mathbf{q}^* \cdot \delta\mathbf{q}^*)$. The former may be expressed by means of (18) and (20), respectively:

$$\delta\mathbf{q}^* \cdot \delta\mathbf{q}^{*\prime} = \beta^2 \left[\delta\hat{\mathbf{q}}' + (\ln\beta)'\,\delta\hat{\mathbf{q}}\right] \cdot \delta\hat{\mathbf{q}} = \beta^2\,(\ln\beta)' \tag{47}$$

In order to reduce the influence of the normalization condition, the ratio

$$\frac{\delta\mathbf{q}^* \cdot \delta\mathbf{q}^{*\prime}}{\delta\mathbf{q}^* \cdot \delta\mathbf{q}^*} = (\ln\beta)' = \frac{\lambda^{*\prime}}{2\,\omega} - \frac{\delta\hat{\mathbf{q}}^T\mathbf{K}_T'\delta\hat{\mathbf{q}}'}{\delta\hat{\mathbf{q}}^T\mathbf{K}_T'\delta\hat{\mathbf{q}}} \tag{48}$$

is computed. It may be used as an indicator for the reliability of *ab initio* estimates of the stability limit. In (48), $(\ln\beta)'$ was expressed by means of (27).

Following the discussion of (46), the bilinear form $\delta\mathbf{q}^{*T}\mathbf{K}_T'\delta\mathbf{q}^{*\prime}$ may take on arbitrary real values. Moreover, it depends on the chosen normalization condition. Based on the explanation of the terms in (46), the following function may be defined:

$$\Psi(\lambda) = \frac{\frac{1}{2}(\delta\mathbf{q}^{*T}\mathbf{K}_T''\delta\mathbf{q}^*)^2 - \frac{1}{\omega}\,\delta\mathbf{q}^{*\prime T}[\mathbf{K}_T + \omega\,\mathbf{K}_T']\delta\mathbf{q}^{*\prime}}{\frac{1}{2}(\delta\mathbf{q}^{*T}\mathbf{K}_T''\delta\mathbf{q}^*)^2 + \frac{1}{\omega}\,\delta\mathbf{q}^{*\prime T}[\mathbf{K}_T + \omega\,\mathbf{K}_T']\delta\mathbf{q}^{*\prime}} \,. \tag{49}$$

In the prebuckling domain, this function maps all possible states $(\omega, \delta\mathbf{q}^*, \delta\mathbf{q}^{*\prime})$ onto the intervall $[-1, 1] \subset \mathbb{R}$. $\Psi = -1$ is related to points characterized by $\lambda^{*\prime} = 0$. The value $\Psi = +1$ is restricted to the stability limit. In chapter 4, it will be demonstrated numerically that, in the aforementioned subregion preceding the stability limit where $\Psi > 0$, the asymptotic properties of the higher-order estimates are characterized by a high degree of high accuracy. It has turned out that this subregion is too small for being of practical use. In other words, defining an estimate of the stability limit as reliable only if $\Psi > 0$ holds, would be too conservative.

An alternative of (48) is obtained in the form of the angle γ enclosed by $\delta\mathbf{q}^*$ and its derivative $\delta\mathbf{q}^{*\prime}$. This cosine is defined as

$$\Omega(\lambda) = \cos\gamma = \frac{\delta\mathbf{q}^{*T}\delta\mathbf{q}^{*\prime}}{\|\delta\mathbf{q}^*\|\|\delta\mathbf{q}^{*\prime}\|} \,. \tag{50}$$

In order to comment on the behavior of $\Omega(\lambda)$, $\delta\mathbf{q}^{*\prime}$ is expressed as

$$\delta\mathbf{q}^{*\prime} = \sum_{j=1}^{N} \alpha_{1j}\delta\mathbf{q}_j^* \,. \tag{51}$$

This is possible since the eigenvectors $\delta\hat{\mathbf{q}} \equiv \delta\hat{\mathbf{q}}_1$ and $\delta\hat{\mathbf{q}}_j$, $j \in \{2, \ldots, N\}$, form a complete basis in $\mathbb{R}^N$. The coefficients of this expansion are obtained as [6]

$$\alpha_{11} = \frac{1}{2}\,\frac{\lambda^{*\prime}}{\omega} \qquad \text{and} \qquad \alpha_{1j} = \frac{\omega}{\omega_j - \omega}\,\frac{\delta\mathbf{q}^{*T}\mathbf{K}_T''\delta\mathbf{q}^*}{\delta\mathbf{q}_j^{*T}\mathbf{K}_T'\delta\mathbf{q}_j^*}, \qquad \forall\, j \geq 2 \quad (\omega_1 \equiv \omega \neq \omega_j) \,. \tag{52}$$

It can be shown, that the coefficients α_{1j}, $j \geq 2$, are zero at bifurcation points whereas $\alpha_{11}|_{\lambda_S} \neq 0$ at that point [6]. Hence, at the stability limit $\delta\mathbf{q}^{*\prime}$ and $\delta\mathbf{q}^*$ are collinear vectors. Hence, (50) yields

$$\lim_{\lambda \to \lambda_S} \Omega = \pm 1 \,. \tag{53}$$

The sign in (53) is identical to the sign of α_{11}. Using results from [8], one obtains

$$\begin{aligned} &\lim_{\lambda \to \lambda_S} \alpha_{11} = -\frac{1}{2}\lambda^{*\prime\prime}|_{\lambda_S} && \text{for bifurcation points,} \\ &\lim_{\lambda \to \lambda_S} \alpha_{11} = -\infty && \text{for snap-through points.} \end{aligned} \tag{54}$$

Substituting these results into (52) and (50), yields

$$\begin{aligned} &\lim_{\lambda \to \lambda_S} \Omega = +1 && \text{for bifurcation points characterized by a local minimum of } \lambda^*, \\ &\lim_{\lambda \to \lambda_S} \Omega = -1 && \text{for bifurcation points characterized by a local maximum of } \lambda^* \text{ and} \\ &\lim_{\lambda \to \lambda_S} \Omega = -1 && \text{for snap-through points.} \end{aligned} \tag{55}$$

For snap-through problems, the negative sign of Ω refers to a subregion of the prebuckling domain before the stability limit, wherein reliable estimates of the stability limit are obtained. This subregion will be found to be larger than the one with $\Psi > 0$. Hence, (50) will be seen to be less conservative than (49).

4. Numerical investigation

The behavior of the estimation functions (eigenvalue functions) λ^*, λ^{**} and $\tilde{\lambda}$ will be investigated by means of a standard problem of shell analysis. It is a shallow cylindrical panel analyzed by Sabir and Lock [16]. Two different thicknesses will be considered. The shell formulation used for the numerical investigation is the one presented by Simo and Fox [17]. The finite element implementation follows the strategy by Simo, Fox and Rifai [19, 18]. Slight modifications of this strategy are described in Helnwein [6]. The mode of computation of the derivatives of $\mathbf{K}_T$ is also explained in that work.

4.1. Shallow cylindrical shell

The shallow cylindrical panel, shown in Fig. 1, was first investigated by Sabir and Lock [16] in 1972. Because of the pronounced nonlinear behavior and the sensitivity of the load–displacement curves with regards to changes of the thickness, this example is a good benchmark for the analysis of shells by means of the FEM.

In this paper, the behavior of the shell as well as the estimation functions for the stability limit will be investigated for a thickness of $t = 12.7\,\text{cm}$ (example 1) and $6.35\,\text{cm}$ (example 2), respectively. Figure 2 shows the load–displacement curves of the points A and B (see Fig. 1) for both examples.

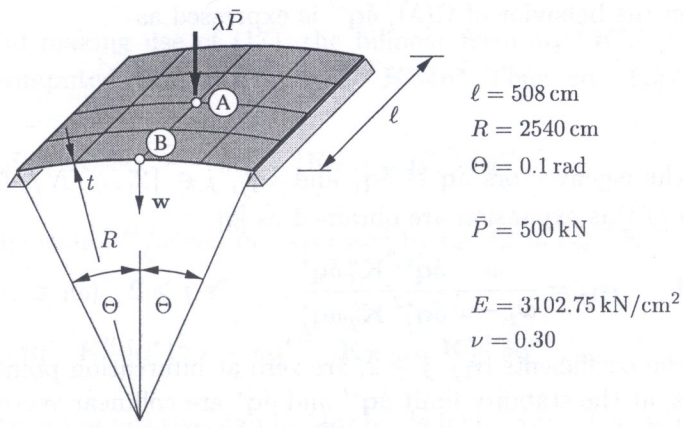

Fig. 1. Geometric and material properties of the shallow cylindrical panel. Definition of the reference load. Location of two characteristic points A and B

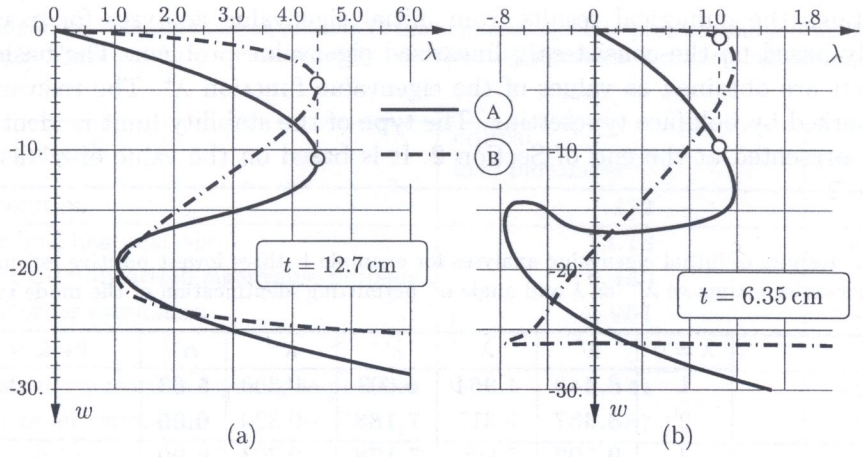

Fig. 2. Load–displacement curves for two characteristic points A and B of the panel. (a) example 1, (b) example 2

Example 1 is characterized by a limit point at $\lambda_S = 4.437$. The primary path is stable in the whole domain $\lambda < \lambda_S$. Example 2 also has a limit point. However, because of the small thickness, a bifurcation point is preceding the limit point. The stability limit is determined by the bifurcation point at $\lambda_S = 1.053$.

4.1.1. Accompanying linear eigenvalue analysis for example 1

The results of an accompanying linear eigenvalue analysis are the eigenvalue function λ^* and the higher-order estimation functions λ^{**} and $\tilde{\lambda}$ for bifurcation and limit points, respectively. The mode of stability limit, estimated by λ_i^*, is identified by means of α_i^* according to (12).

Figure 3 shows the estimation function λ^* and the corresponding higher-order estimates for example 1. The function values at $\lambda = 0$ are marked by circles (λ^*), triangles (λ^{**}) and by a square ($\tilde{\lambda}$). These values are the results of so-called *initial eigenvalue analyses*. For these analyses, the eigenshapes (buckling-mode, described by $\delta\mathbf{q}^*$) corresponding to the three lowest positive values of λ^* are plotted in Fig. 3.

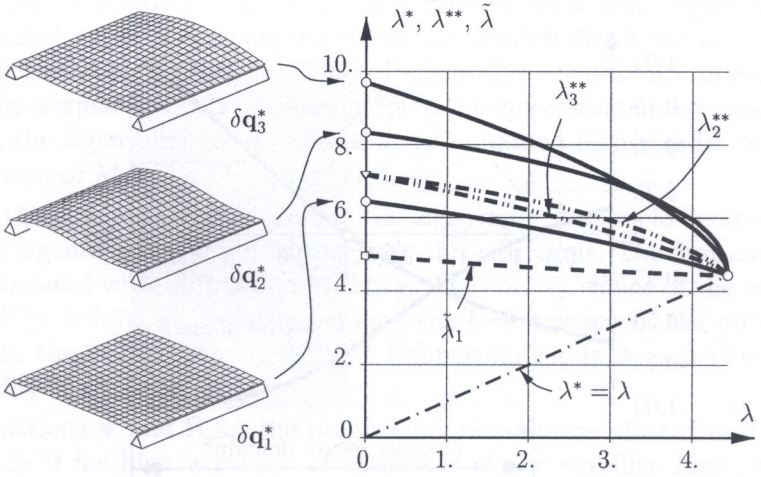

Fig. 3. Eigenvalue functions for the three lowest positive values of λ^* and higher-order estimation functions; the plotted buckling modes are estimates obtained from initial eigenvalue analysis

Table 2 contains the numerical results from initial eigenvalue analyses for example 1. These results are solely based on the consistently linearized eigenvalue problem. The basic estimates for the stability limit are obtained as values of the eigenvalue function λ^*. The relevant higher-order estimates are marked by boldface typesetting. The type of the stability limit is identified according to the criterion presented at the end of Section 2. It is based on the value of α^* listed in the last column of Table 2.

Table 2. Results of initial eigenvalue analyses for example 1: three lowest positive estimates λ^*, higher-order estimates λ^{**} or $\tilde{\lambda}$ and angle α^* permitting identification of the mode type

$\lambda = 0$	λ^*	$\tilde{\lambda}$	λ^{**}	$\lambda^{*\prime}$	α^*
1	**6.449**	**4.961**	5.608	−0.300	**5.63**
2	**8.337**	6.317	**7.188**	−0.320	**0.00**
3	**9.702**	5.696	**7.178**	−0.703	**0.00**

The lowest value of the load assessed by means of the higher-order estimation functions is assumed to be associated with the critical buckling mode. For the current problem, this is the first mode, i.e., $\delta\mathbf{q}_1^*$ in Fig. 3. Moreover, this mode indicates that loss of stability will occur at a snap-through point. This agrees with the result obtained from a fully non-linear analysis using an arc-length technique.

In order to prove the suitability of the eigenvalue estimation and the relevant higher-order estimates, the indicator functions Ψ and Ω are evaluated for the initial state. Moreover, for the purpose of investigating the behavior of the estimation functions as well as that of Ψ and Ω for an accompanying eigenvalue analysis, the indicator functions are computed and plotted in Fig. 4. According to the criterion given in the course of the explanation of (49), estimates of high accuracy should be obtained for $\lambda \geq \lambda|_{\Psi=0} = 2.45$.

Since the critical buckling-mode for example 1 is associated with a snap-through point, the third relation in (55) may serve as a suitable criterion for estimates of high accuracy. Thus, according to the condition for high accuracy estimates, i.e., if $\Omega < 0$, such estimates should be obtained for $\lambda \geq \lambda|_{\Omega=0} = 0.75$.

Table 3 lists the relative error of different types of estimates for the stability limit, i.e., of the load level related to the snap-through point. It contains results from initial eigenvalue analysis ($\lambda = 0$), and from computations at $\lambda|_{\Psi=0} = 2.45$ and $\lambda|_{\Omega=0} = 0.75$. The relative error listed in the last column demonstrates that a *linear buckling analysis* is of no use for snap-through problems. This was previously pointed out and discussed by the authors in [9] and [10].

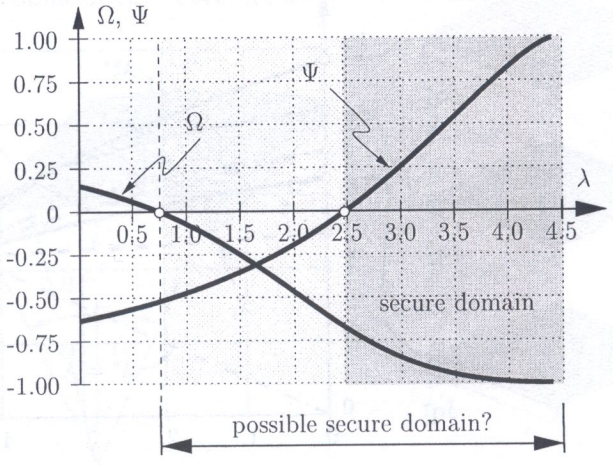

Fig. 4. Indicator functions Ψ and Ω as functions of the load parameter λ. Evaluated for example 1 ($t = 12.7$ cm)

Table 3. Comparison between the true solution of the nonlinear stability problem and solutions obtained from linear buckling analysis and from the consistently linearized eigenproblem including higher-order estimates for example 1

Used approach	critical load parameter	rel. error
True solution	**4.432**	—
Linear buckling analysis	**13.16**	**+197 %**
Consistently linearized eigenvalue problem	**6.449**	**+45 %**
Higher-order estimation	**4.961**	**+12 %**
$\lambda\|_{\Psi=0} = \mathbf{2.45}$		
Consistently linearized eigenvalue problem	**5.541**	**+25.0 %**
Higher-order estimation	**4.587**	**+3.5 %**
$\lambda\|_{\Omega=0} = \mathbf{0.75}$		
Consistently linearized eigenvalue problem	**6.201**	**+39.9 %**
Higher-order estimation	**4.830**	**+9.0 %**

The results obtained by means of solving the consistently linearized eigenvalue problem are remarkably better than those obtained from a linear buckling analysis. Nevertheless, only the higher-order estimates yield results with acceptable accuracy.

As regards $\Psi > 0$ as a criterion for high accuracy, Ψ only becomes positive at approximately 55 % of λ_s. The respective relative error of only +3.5 % shows that this indicator is somewhat too conservative for engineering purposes.

As regards $\Omega < 0$ as an indicator for high accuracy of estimates of snap-through points, Ω becomes negative of approximately 0.167 λ_s. The corresponding relative error of +9.0 % is acceptable for many engineering applications.

4.1.2. Accompanying linear eigenvalue analysis for example 2

This example refers to the thinner shell ($t = 6.35$ cm). Hence, the influence of geometric nonlinearity is stronger than for example 1. Moreover, the type of the stability limit changes from snap-through to bifurcation. Figure 2(b) shows load–displacement curves for two characteristic degrees of freedom, i.e., the vertical deflections of the points A and B (see in Fig. 1).

Figure 5 shows the estimation function λ^* and the corresponding higher-order-estimates for the stability limit based on an accompanying eigenvalue analysis with the help of the consistently linearized eigenvalue problem. Results from initial eigenvalue analysis are marked by circles (λ^*), triangles (λ^{**}) and by a square ($\tilde{\lambda}$). As a consequence of the more pronounced geometric nonlinearity than for example 1, the eigenvalue curves as well and the related higher-order estimation functions are (with the exception of $\lambda_S^*(\lambda)$) no longer monotonic.

Table 4 contains the numerical results from initial eigenvalue analysis for example 2. Based on the angle α^*, the second eigenmode is identified as a snap-through mode. The first and third eigenmode, respectively, are associated with bifurcation buckling. The correct choice of the related higher-order estimates is marked by boldface typesetting. Using the lowest value of the obtained higher-order estimates to indicate the critical mode, the first bifurcation mode is recognized to be the mode leading to the stability limit.

The indicator functions Ψ and Ω for the prebuckling domain are plotted in Fig. 6. On the basis of the condition $\Psi > 0$ for high accuracy of estimates of the stability limit, accurate estimates are obtained only in a small domain before the stability limit. It is remarkable that the indicator function Ψ reaches the limiting value of Ψ, i.e., $\lim_{\lambda \to \lambda_S} \Psi = +1$, with a steep slope. For snap-through problems, $d\Psi/d\lambda$ is zero at the stability limit (see Fig. 4).

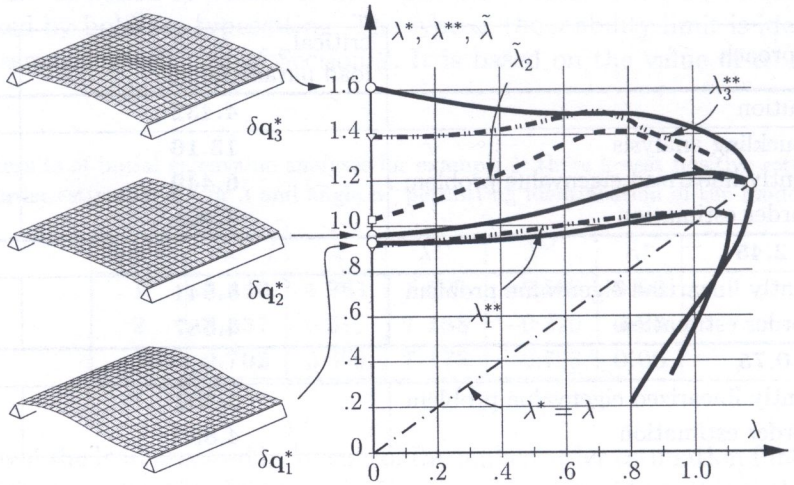

Fig. 5. Eigenvalue functions for the three lowest positive values of λ^* and higher-order estimation functions; the plotted buckling modes as estimates obtained from initial eigenvalue analysis

Table 4. Results of initial eigenvalue analyses for example 2: three lowest positive estimates λ^*, higher-order estimates λ^{**} or $\tilde{\lambda}$ and angle α^* permitting idenification of the mode type

$\lambda = 0.00$	λ^*	$\tilde{\lambda}$	λ^{**}	$\lambda^{*\prime}$	α^*
1	**0.927**	0.903	**0.915**	−0.027	**0.00**
2	**0.959**	**1.029**	0.993	0.068	**9.05**
3	**1.615**	1.230	**1.396**	−0.313	**0.00**

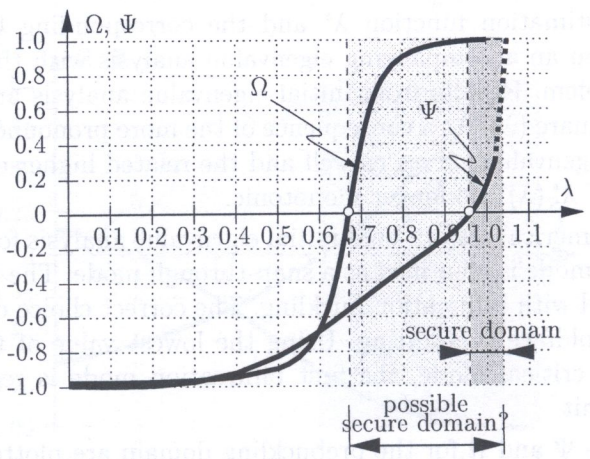

Fig. 6. Indicator functions Ψ and Ω as functions of the load parameter λ. Evaluated for example 2 of the shell geometry ($t = 6.35$ cm)

According to (55), the sign of Ω is not an indicator of the proximity of the stability limit, if this limit is a bifurcation point as in the case for example 2. Nevertheless, it may be of interest to trace the sign of Ω while tracing the nonlinear load–displacement path. The point at which Ω changes its sign may yield a less conservative indicator.

Table 5 contains a summary of relative errors obtained from initial eigenvalue analysis and from computation at $\lambda|_{\Psi=0} = 0.96$ and $\lambda|_{\Omega=0} = 0.67$. The relative error of the *linear buckling analysis* is significantly smaller than the one observed for snap-through problems. This is in perfect agreement to observations concerning beam structures as discussed in [10]. Nevertheless, none of the estimates based on the consistently linearized eigenvalue problem show a relative error as large as the one from a *linear buckling analysis*.

Table 5. Comparison of the true solution of a nonlinear stability problem with results from linear buckling analysis and from the consistently linearized eigenproblem including higher-order estimates for example 2

Used approach	critical load parameter	rel. error
True solution	**1.050**	—
Linear buckling analysis	**1.351**	**+29 %**
Consistently linearized eigenvalue problem	**0.924**	**−13 %**
Higher-order estimation	**0.900**	**−14 %**
$\lambda\|_{\Psi=0} = 0.96$		
Consistently linearized eigenvalue problem	**1.041**	**−0.9 %**
Higher-order estimation	**1.049**	**−0.1 %**
$\lambda\|_{\Omega=0} = 0.67$		
Consistently linearized eigenvalue problem	**0.975**	**−7.1 %**
Higher-order estimation	**1.012**	**−3.6 %**

A critical investigation of the estimates obtained at $\lambda|_{\Psi=0} = 0.96 \approx 0.91\ \lambda_S$ shows that the criterion $\Psi \geq 0$ is too conservative for bifurcation problems. Using the analysis at $\lambda|_{\Omega=0} = 0.67 \approx 0.64\ \lambda_S$, i.e., at the point of the sign change of Ω, the obtained relative error of -3.6 % seems to be a good choice for engineering purposes. The usefulness of this choice is verified by means of Fig. 5: In the domain defined by $\lambda|_{\Omega=0} \leq \lambda \leq \lambda_S$, the eigenvalue curve λ^* as well as the higher-order estimate $\tilde{\lambda}$ uniformly tend to the stability limit $\lambda_S = 1.050$.

Thus, with regards to bifurcation buckling, the domain between the point at which Ω changes its sign and the stability limit appears to be reliable as far as estimates of this limit are concerned.

5. Conclusions

In this paper an overview on estimation functions for stability limits on non-linear load displacement paths of elastic structures under static loads was given. The estimation functions used in this paper are based on the so-called consistently linearized eigenvalue problem.

Since such estimation functions are suitable only in an asymptotic sense, indicator functions for the assessability of the stability limit by means of the previously mentioned estimation functions were presented. The suitability of such indicator functions was demonstrated numerically. It was shown that the presented indicator functions provide additional information on the sensitivity of numerical estimations for the stability limit.

For snap-through problem, reliable estimates of the stability limit are obtained within a subdomain preceding the stability limit, which is characterized by $\Omega > 0$. As regards bifurcation buckling, reliable estimates of the stability limit are obtained at and after the point at which Ω changes its sign. $\Psi \geq 0$ was shown to be too conservative a criterion for reliable estimates of bifurcation points.

REFERENCES

[1] K.J. Bathe. *Finite Element Procedures.* Prentice Hall, Englewood Cliffs, New Jersey, 2nd edition, 1996.

[2] B. Brendel. *Geometrisch nichtlineare Elastostatik* (in German). Dissertation, Universität Stuttgart, Deutschland, Institut für Baustatik, 1979.

[3] B. Brendel, E. Ramm, F.D. Fischer, and F.G. Rammerstorfer. Linear and nonlinear stability analysis of thin cylindrical shells under wind loads. *Structural Mechanics*, **9**: 91–113, 1981.

[4] D. Bushnell. Stress, stability and vibration of complex branched shells of revolution: Analysis and user manual for BOSOR 4. *NASA CR-2116*, 1972.

[5] R.H. Gallagher and H.T.Y. Yang. Elastic instability predictions for doubly-curved shells. In *Proceedings of the 2nd Conference on Matrix Methods in Structural Mechanics*, 711–739, Wright–Patterson A.F. Base, Ohio, 1968.

[6] P. Helnwein. *Zur initialen Abschätzbarkeit von Stabilitätsgrenzen auf nichtlinearen Last-Verschiebungspfaden elastischer Strukturen mittels der Methode der Finiten Elemente* (in German). Dr.-techn.-thesis, Vienna University of Technology, Institute for Strength of Materials, 1996.

[7] P. Helnwein. *Begleitende lineare Eigenwertanalysen für Stabilitätsprobleme mit geometrisch nichtlinearem Vorbeulpfad – Eine numerische Untersuchung mittels der FEM* (in German). Dipl.-Ing.-thesis, Vienna University of Technology, Institute for Strength of Materials, 1991.

[8] P. Helnwein and H. A. Mang. An asymptotic approach for the evaluation of errors resulting from estimations of stability limits in nonlinear elasticity. *Acta Mechanica*, **125**: 235–254, 1997.

[9] P. Helnwein and H.A. Mang. Bewertung begleitender Eigenwertanalysen zur Abschätzung von Stabilitätsgrenzen von Problemen der nichtlinearen Elastizitätstheorie (in German). *Zeitschrift für Angewandte Mathematik und Mechanik*, 78(2):S473–474, 1998.

[10] P. Helnwein and H.A. Mang. "Der Blick über den Zaun" – Lineare Stabilitätsuntersuchungen als Träger von Informationen über nichtlineares Strukturverhalten im Vorbeulbereich (in German). *Der Bauingenieur*, 73(5):247–256, 1998.

[11] R.H. Mallet and P.V. Marçal. Finite element analysis of nonlinear structures. *J. Struct. Div. Proc. ASCE*, **94**: 2081–2105, 1968.

[12] H.A. Mang and P. Helnwein. Lower and upper bounds for stability limits on geometrically nonlinear prebuckling paths. In S. Valliappan, V.A. Pulmano, and F. Tin-Loi, eds., *Proceedings of the Second Asian-Pacific Conference on Computational Mechanics*, 157–164, Sydney, Australien, 3.–6. August 1993. Balkema, Rotterdam–Boston.

[13] H.A. Mang and P. Helnwein. A priori estimates of stability limits on nonlinear load-displacement paths. In J.B. Obrębski, ed., *Proceedings of the International Conference on Lightweight Structures in Civil Engineering*, **II**: 811–821, Warschau, Polen, 25–29 September 1995. Magat Warschau.

[14] H.A. Mang and P. Helnwein. Second-order a-priori estimates of bifurcation points on geometrically nonlinear prebuckling paths. In S.N. Atluri, G. Yagawa, and T.A. Cruse, eds., *Computational Mechanics '95. Proceedings of the International Conference of Computational Engineering Science*, **II**: 1511–1516, Hawaii, USA, 30. Juli–3. August 1995. Springer, Berlin.

[15] B. Pichler. *Zur Zuverlässigkeit initialer Abschätzungen von Stabilitätsgrenzen auf nichtlinearen Last-Verschiebungspfaden elastischer Strukturen mittels der Methode der Finiten Elemente* (in German). Diploma thesis, Vienna University of Technology, Austria, 1998.

[16] A.B. Sabir and A.C. Lock. The application of finite elements to the large deflection geometrically nonlinear behaviour of cylindrical shells. In *Variational Methods in Engineering*, **7**: 66–75, Southhampton, 1972. University Press.

[17] J.C. Simo and D.D. Fox. On a stress resultant geometrically exact shell model. part I: Formulation and optimal parametrization. *Computer Methods in Applied Mechanics and Engineering*, **72**: 267–304, 1989.

[18] J.C. Simo, D.D. Fox, and M.S. Rifai. On a stress resultant geometrically exact shell model. Part II: The linear theory; computational aspects. *Computer Methods in Applied Mechanics and Engineering*, **73**: 53–92, 1989.

[19] J.C. Simo, D.D. Fox, and M.S. Rifai. On a stress resultant geometrically exact shell model. Part III: Computational aspects of the nonlinear theory. *Computer Methods in Applied Mechanics and Engineering*, **79**: 1–62, 1990.

[20] H. Troger and A. Steindl. *Nonlinear Stability and Bifurcation Theory.* Springer, Wien, 1991.